

DOI: 10.24425/123845

L. RAKOCZY*[#], M. GRUDZIEN**[#], R. CYGAN***[#], A. ZIELIŃSKA-LIPIEC***EFFECT OF COBALT ALUMINATE CONTENT AND POURING TEMPERATURE ON MACROSTRUCTURE, TENSILE STRENGTH AND CREEP RUPTURE OF INCONEL 713C CASTINGS**

The effect of cobalt aluminate inoculant addition and melt-pouring temperature on the structure and mechanical properties of Ni-based superalloy was studied. The first major move to control the quality of investment cast blades and vanes was the control of grain size. Cobalt aluminate (CoAl_2O_4) is the most frequently utilized inoculant in the lost-wax casting process of Ni-based superalloys. The inoculant in the prime coat of moulds and pouring temperature play a significant role in grain size control. The finest surface grains were obtained when the internal surface of shell mould was coated with cobalt aluminate and subsequently pouring was at 1480°C . The influence of selected casting parameters and inoculant addition on mechanical properties was investigated on the basis of tensile, creep and hardness testing. The effect of grain refinement on mechanical properties were consistent with established theories. Tests conducted at ambient temperature indicated a beneficial effect of grain refinement both on tensile strength and hardness. In contrast at elevated temperature during creep, the reverse trend was observed.

Keywords: pouring, investment casting, lost wax, superalloy, creep

1. Introduction

Inconel 713C belongs to the group of nickel based alloys which are characterized by an unique combination of properties at elevated temperatures. High mechanical properties, excellent resistance to oxidation and hot corrosion make them suitable to manufacturing components in jet engines and industrial gas turbines [1-3]. The usefulness of superalloys for harsh environment applications is given by few physical factors. Face centered cubic (FCC) crystallographic system is characterized by low rates of thermally activated processes and so creep deformation is relatively small. Furthermore, this polymorph is thermodynamically stable from liquid nitrogen temperature up to the melting point; thus phase transformations of γ -matrix do not occur. Nickel is able to promote the precipitation of the intermetallic phase $\text{Ni}_3(\text{Al}, \text{Ti})$, denoted as γ' , which exhibits the L1_2 crystal structure. In doing so, the so-called yield stress anomaly arises: the flow stress rises with temperature, an effect exploited for high temperature components [4-6]. Inconel 713C is widely used in the production of low pressure turbine (LPT) blades and vane clusters. Due to high costs of machining, investment casting is a fundamental method for the fabrication of parts with complex geometries. Exceptional properties are gained with the lost wax process, especially high dimensional accuracy due to monolithic ceramic moulds, and better metallurgical features originating

from the use of preheated moulds [7]. Cost disparity between investment casting and other casting methods results from the necessity to create expendable patterns and construct individual moulds from these. The primary field for investment casting of Inconel 713C is the production blades and vane clusters, usually for low pressure turbine (LPT) section. This specialized area of investment casting technology demands various processing techniques to provide the high metallurgical quality in critical gas turbine components [8]. Development over the years in the complexity and integrity of lost-wax castings has led a continuous improvement in capability of the manufacturing process. Superior mechanical properties of nickel based superalloy generally originate also from alloying elements in Ni-matrix and properly conducted heat treatment, namely solution and ageing [9]. It is noteworthy that the high resistance to creep and low cycle fatigue of Inconel 713C alloy are sufficiently achievable in the "as cast state", thus costly heat treatment is eliminated [10]. Development in the manufacturing technology to attain the highest properties requires intensive investigations and testing. For this reason it is important to make a correlation between process parameters, constituents in the shell mould and mechanical properties of Inconel 713C in as cast condition. Continuous improvement of engines makes the LPT section much more complex in structure. Service temperature reaches even 700°C and so fine grained microstructure characterized by high

* AGH UNIVERSITY OF SCIENCE AND TECHNOLOGY, FACULTY OF METALS ENGINEERING AND INDUSTRIAL COMPUTER SCIENCE, DEPARTMENT OF PHYSICAL AND POWDER METALLURGY, AL. MICKIEWICZA 30, 30-059 KRAKÓW

** FOUNDRY RESEARCH INSTITUTE, 73 ZAKOPIAŃSKA STR., 30-418 KRAKÓW, POLAND

*** CONSOLIDATED PRECISION PRODUCTS POLAND, 120 HETMAŃSKA STR., 35-078 RZESZÓW, POLAND

Corresponding author: lrakoczy@agh.edu.pl

strength is required. However, it is important to remember that the grain refinement leads to a decrease in creep resistance. High strength is favoured by fine grain size, in turn creep favoured by coarse grain size, so optimum range of sizes is required by end users. Cast components operating in the turbine, due to service conditions, must have appropriate microstructure and lack casting defects that can contribute to catastrophic failure. Mentioned features can be controlled by melt-pouring temperature and composition of the prime coat [11]. Filling ability of thin wall blades and vanes can be improved through increase of pouring temperature, however on the other hand, it leads to grain coarsening. In the LPT section operating temperature is usually below the creep range, and so stresses originating from centrifugal loads are relatively low [12]. In order to overcome this problem, castings are usually modified by the addition of refiners which contain high stability particles or adding inoculant to the prime coat of the ceramic mould. Grain refinement of the cast microstructure is directly connected with increasing the heterogeneous nucleation sites during solidification [13]. Some information is available in the literature [10,14-16] about modification of Inconel 713C superalloy, but the aviation industry continues to seek new solutions and improvements to increase durability of critical components, also called flight safety parts. The effect of the selected process parameters, geometry of castings as well as the preparation of ceramic mould on the mechanical properties of the Inconel 713C superalloy, presented in this work, has not yet been analyzed. The aim of the investigation was to establish the influence of the CoAl_2O_4 content in the prime coat and melt-pouring temperature on the macrostructure, microstructure and also mechanical properties at room and elevated temperatures.

2. Experimental procedure

Four Inconel 713C investment castings with different pouring temperatures and prime coatings of shell mould were fabricated. The superalloy used in this experiment was provided by Canon Muskegon Company. The wax patterns were injection moulded and then ceramic monolithic mould was built up around these patterns by a series of dip coatings. Two prime coats were produced for the casting:

- Shell mould 1-2: The prime coat consisted zircon filler and colloidal silica binder,
- Shell mould 3-4: Similar to 1-2 plus 5 wt. % of CoAl_2O_4 inoculant.

Grit of alumina was used as a primary stucco, and then few coat mould backups made of ceramic slurries based on alumina silicate powders and colloidal silica binder. As a backup stucco aluminate silicate grit was used. One of prepared shell mould is shown in Fig. 1. The wax patterns were removed from the shell molds in boilerclave and then covered with alumina silicate Fiberfrax® insulation. Whole assemblies were fired in air in order to harden the moulds. Master heat charges were melted in a zirconia crucible mounted in the VIM IC Consarc furnace. Directly before melting the moulds were preheated up

to 1000°C. During melting and subsequent pouring, the vacuum was 2×10^{-3} mbar. Two melt-pouring temperatures, controlled by Pt/Pt-Rh thermocouples, were selected: 1480°C (shell 1, 3) and 1520°C (shell 2, 4).



Fig. 1. One of the shell mould prepared in the experiment

TABLE 1

Experimental conditions

Content of inoculant [wt. %]	Preheat temperature [°C]	Melt pouring temperature [°C]	
		1480	1520
		Description of shell	
0	1000	N1	N2
5	1000	M1	M2

After the alloy has solidified and cooled, the moulds were broken away and the castings subjected to further investigation. The geometry of cast element after excision from assembly and machining is presented in Fig. 2. Measuring length is equal 32 mm.



Fig. 2. Geometry of prepared element after: a) excision b) machining

In order to establish influence of inoculant content and melt-pouring temperature on mechanical properties and macrostructure of Inconel 713C, light microscopy and scanning electron microscopy observations were made, and creep, tensile and hardness testing were performed. Chemical composition of the alloy was estimated by Optical Emission Spectroscopy (OES) and the results are included in Table 2.

TABLE 2
Chemical composition of Inconel 713C

Element	Cr	Al	Mo	Nb	Ti	Co	C	Zr	Ni
Wt. [%]	13.31	6.13	4.20	2.45	0.89	0.27	0.12	0.08	Bal.

Samples for macroscopic and microscopic examinations of base metals were taken from the top surface of the cast elements. Afterwards they were mounted in resin, metallographically prepared (grinding, polishing) and finally chemically etched in AG21 (macro) and no. 17 Etch (micro) reagents. Macroscopic and microscopic observations were conducted on Nikon, Leica and FEI devices. Tensile tests were performed at ambient temperature according to ASTM E8M-13a standard on an INSTRON 3382 device. Vickers hardness was measured in accordance with the requirements of PN EN ISO 6507-1. Creep tests were carried out on Walter+Bai AG LFMZ-30 machine in accordance to the requirements of ASTM E139 standard. Specimens were heated up to 982°C with a final holding time 60 minutes. Subsequently they were loaded with an axial force which produces on their cross sections an initial tensile stress of 151.8 MPa.

3. Results

3.1. Macro and microstructure

The macrostructures representative different as cast samples are presented in Fig. 3. The results of the grain size analysis depending on pouring temperature and content of cobalt aluminate are shown in Table 3. It is to be noted that the increase in the melt-pouring temperature leads to grain growth due to the lower cooling rate of the crystallization process. The increase in pouring temperature by 40°C (N1→N2) results in an increase in the average surface of grain by more than 70%, thus decreasing the number of grains per millimeter. Captured images indicate that a 5% addition of cobalt aluminate is a great modifier for this Ni-based superalloy. Surface modification conducted at 1480°C led to a 2.6-fold decrease in the average surface of grain from 6.42 mm² to 2.44 mm². For the modified and non-modified alloy the number of grains per square millimeter was 0.16 and 0.41, respectively.

TABLE 3
Stereological parameters of non-modified and modified alloys

Variant	N1	M1	N2	M2
Average surface of grain [mm ²]	6.42	2.44	11.03	5.56
Number of grains per mm ²	0.16	0.41	0.09	0.18

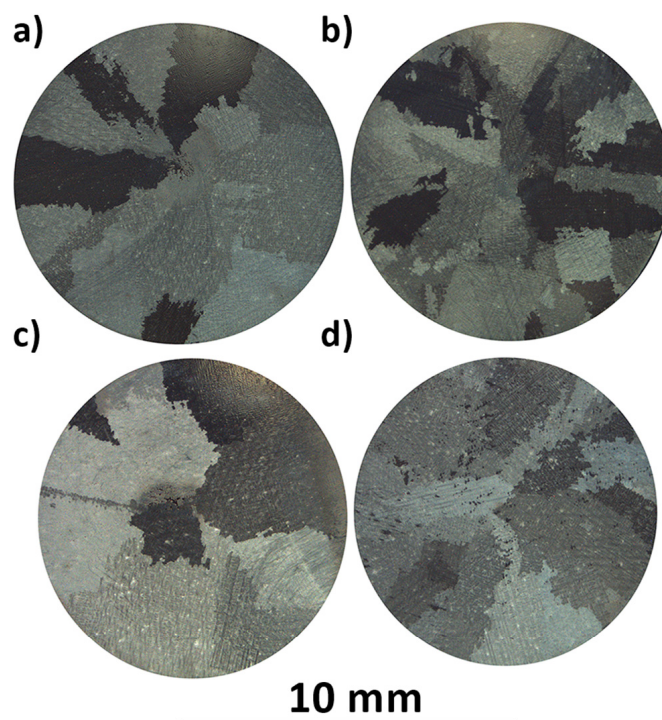


Fig. 3. Macrostructure of prepared castings: a) N1; b) M1; c) N2; d) M2

The average surface of the grain size of the specimen cast at 1520°C was 11.03 mm². Addition of 5% of cobalt aluminate to the prime coat caused an almost twice decrease to 5.56 mm². In the first case (sample N2), the number of grains per unit area was 0.09 and in the second (sample M2), the value was twice as high. Analysis of the macrostructures for casting defects showed that the unmodified samples (coarse grained) exhibited higher porosity. It is important to emphasize that in the prepared castings chill zone structure, which is generally unacceptable, was not observed.

Regardless of the pouring temperature and the inoculant addition inside the equiaxed grains a dendritic structure with high local inhomogeneity was observed. Example of the microstructure of as-cast Inconel 713C is shown in Fig. 4. Segregation of alloying elements occurs during solidification of casting (Fig. 4a). Dissimilarity between microstructure of dendrite core and interdendritic spaces originates from decrease of solubility of elements in γ -matrix during cooling. The main strengthening phase γ' is surrounded by matrix fulfill cores, in turn enrichment of interdendritic spaces with elements additionally caused formation of γ/γ' eutectic island and carbides (Fig. 4b). In dendrite cores intermetallic phase γ' has a cubic shape, whereas in eutectic particles it is more globular. Interdendritic regions are strongly enriched in niobium, and so carbides precipitated mainly in these areas. Fig. 4c shows a scanning electron microscopy microstructure with marked field of EDS analysis. In Fig. 4d and 4e EDS spectra originating from the dendrite core and MC-type primary niobium rich carbide are presented. Carbides assumed different morphology from the blocky-shape, through the parallelograms, to the characteristic shape referred to in the literature as Chinese script. Dendrite cores are enriched in Cr and Mo which suggest that during solidification these elements likely segregate into γ .

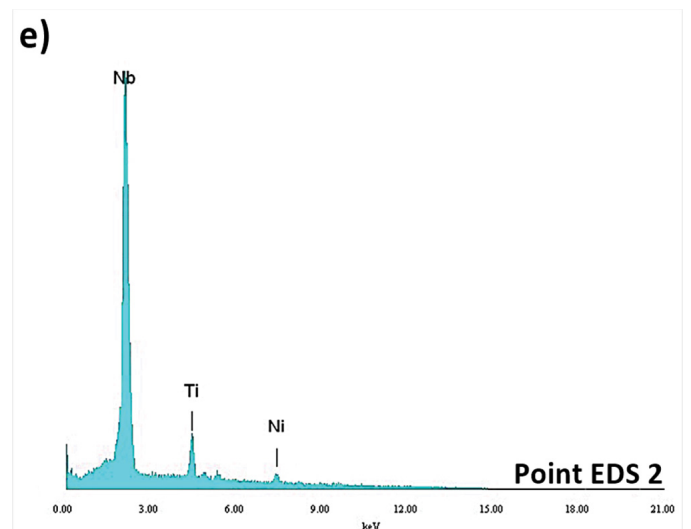
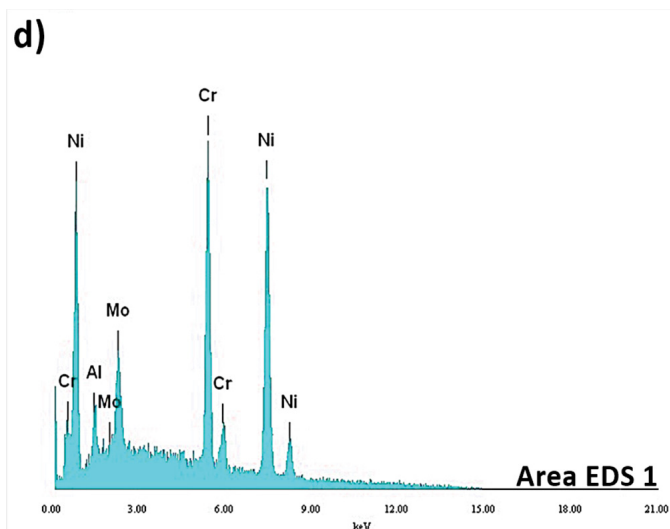
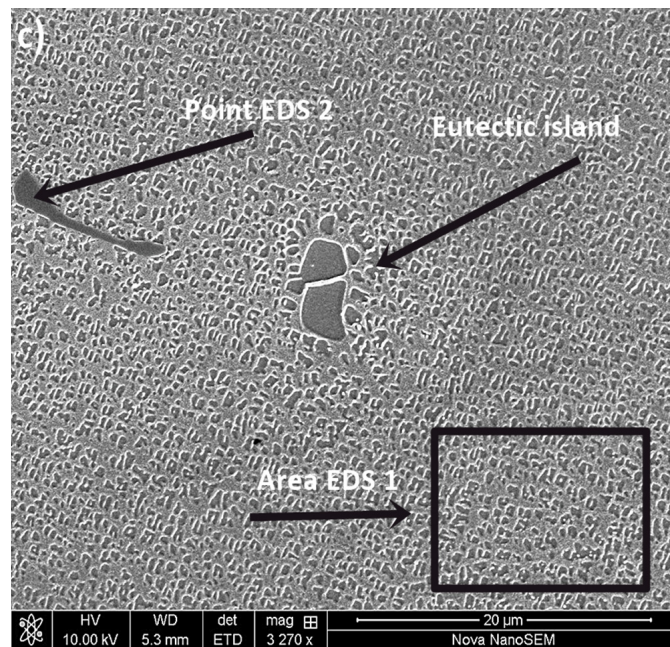
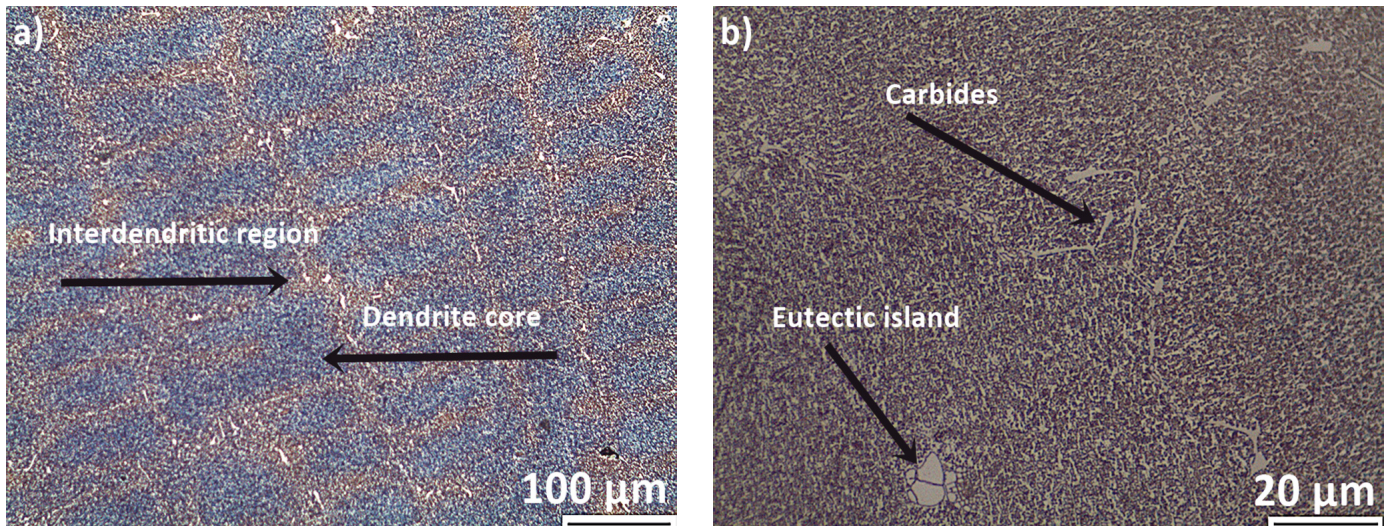


Fig. 4. Inconel 713C structure in the as cast state: a) dendritic structure; b) eutectic γ/γ' island and carbides; c) location of EDS analysis regions; d) EDS spectrum of the dendrite core; e) EDS spectrum of a Nb-rich carbide

3.2. Mechanical properties

Stress-strain curves obtained during tensile testing at ambient temperature are presented in Fig. 5. All the test results are shown in Table 4. Irrespective of the melt-pouring temperature, similar yield strength results were obtained for unmodified and surface modified samples. The addition of cobalt aluminate to prime coat improved the yield strength by 70 MPa for 1480°C and 72 MPa for 1520°C, which is almost identical. A slightly larger difference in the obtained values was observed for the ultimate tensile strength.

The results indicate that maximum values of ultimate tensile strength and strain are achieved for modified castings. Sample M1 broke at stress 1030 MPa, i.e. at 104 MPa greater than sample N1. The surface modification subjected for the 1480°C pouring temperature increased the UTS by 11%. The values obtained for samples poured at 1520°C were slightly lower and were respectively 861 MPa for the unmodified sample and 980 MPa for the sample with CoAl_2O_4 addition. An addition of inoculant to prime coat and pouring temperature of 1480°C consequently attained the optimal combination of mechanical properties.

Macrostructure of the fractures and their cross-sections after a tensile test, are shown in Fig. 6 and 7. The complex character of cracking was observed and it indicates structural heterogeneity of the cast superalloy. Cracks propagated through equiaxed grains of the castings along the interdendritic areas. Few secondary cracks were observed, namely two on the inner surface of sample M1 and one inside of sample N2.

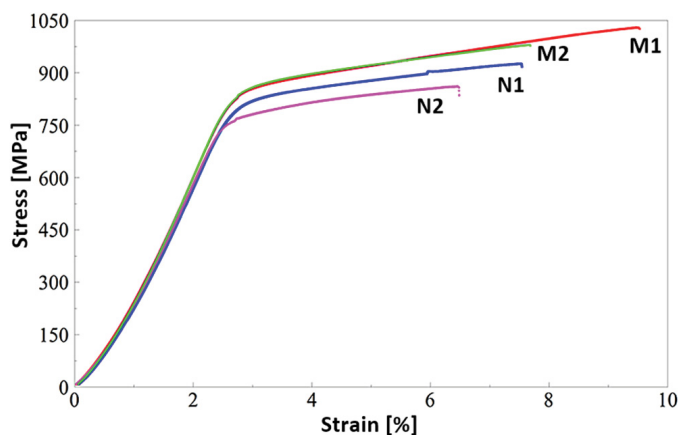


Fig. 5. Tensile testing curves

TABLE 4

Ambient temperature tensile test results of Inconel 713C

Pouring Temperature [°C]	Content of inoculant [%]	Description	Yield strength 0.2% [MPa]	Tensile strength [MPa]
1480	0	N1	750	926
1480	5	M1	820	1030
1520	0	N2	749	861
1520	5	M2	821	980

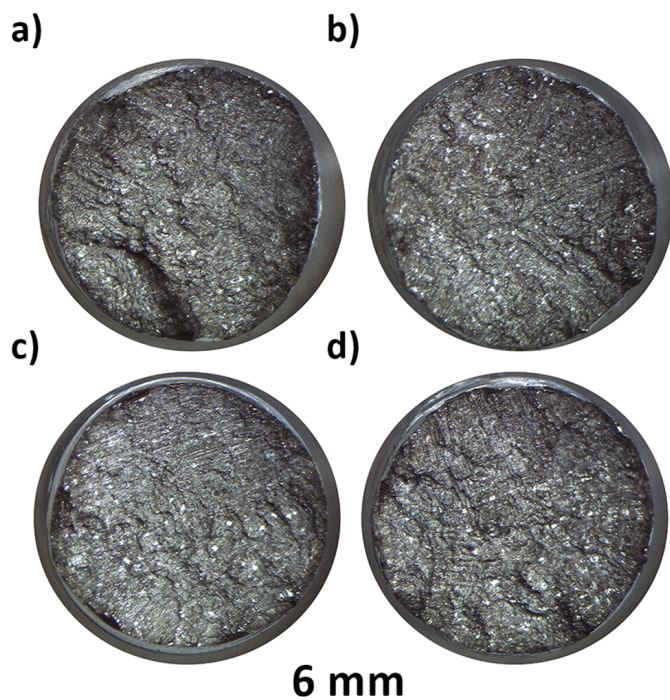


Fig. 6. Fractures of tensile test specimens: a) N1; b) M1; c) N2; d) M2

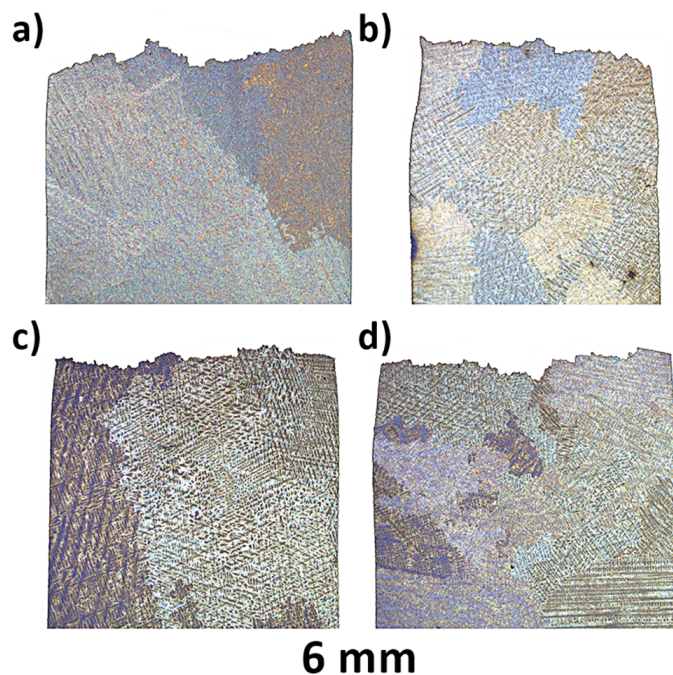


Fig. 7. Cross sections of tensile test fractures: a) N1; b) M1; c) N2; d) M2

At high temperature/low stress (e.g. 982°C/151.8 MPa), superalloys show steady creep with a short primary stage and steady state represented by a plateau and pronounced strain appearing at the tertiary stage. Fig. 8 shows the percentage strain as a function of rupture time, creep curves have the classical shape, while the detailed results are in Table 5. It was noted that Inconel 713C modified with cobalt aluminate independently of the melt-pouring temperature, showed lower rupture life comparison with the unmodified alloy. For the specimens poured from 1520°C,

the decrease was almost 10%, while for the specimens poured from 1480°C more than 11%. Time to rupture of sample M1 was 4.8 h shorter in comparison with sample N1 (41.4 h), in turn for sample M2 poured from the higher temperature, time to rupture was 38.1, and so 4.2 h shorter than for non-modified specimen. The shorter time to rupture results essentially from grain refinement, because the surface areas of the grain boundaries being the preferred deformation sites during creep and creep rate is increased. The longest time to fracture was 42.3 h for the sample N2, and the shortest 36.6 h for the M1 variant. Materials characterized by coarse grains withstood the applied stress the longest time. Creep rate in steady state is increase with grain refinement for both melt-pouring temperatures. At 1480°C creep rate for sample N1 is equal 0.035% per hour, whereas modification increases this rate by more than 40%. At 1520°C creep rates both modified and non-modified samples are close with a little higher value for the fine-grain specimen.

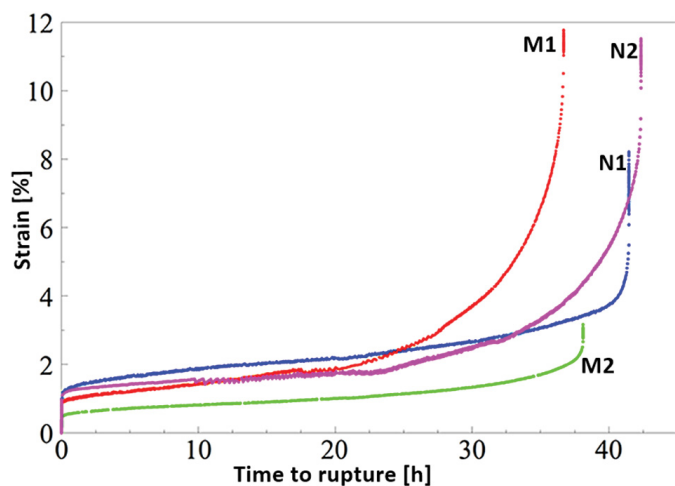


Fig. 8. Creep curves

TABLE 5

Creep resistance of Inconel 713C

Pouring Temperature [°C]	Content of inoculant [%]	Description	Time to rupture [h]	Steady state creep rate [%/h]
1480	0	N1	41.4	0.035
1480	5	M1	36.6	0.050
1520	0	N2	42.3	0.022
1520	5	M2	38.1	0.025

Fig. 9 and 10 show macrostructures of the fractures and cross sections, respectively of the specimens after stress rupture. The test was carried out at a temperature of nearly 1000°C (above potential service temperature) in air, so an oxide layer was observed on the fractures. Dark green colouration indicates the formation of chromium rich oxide on their inner area. Fractures are characterized by a highly developed surface due to uneven plastic deformation. The cross-sectional microstructures show the intergranular fracture mode. In the N1 sample, the grains are larger than in the sample M1; direction of the crack propaga-

tion indicates that relatively high “jumps” are associated with separation of larger grains. Similar tendency occurs in N2 and M2 samples. There are also numerous secondary cracks that have been initiated and run along the inside of the material,

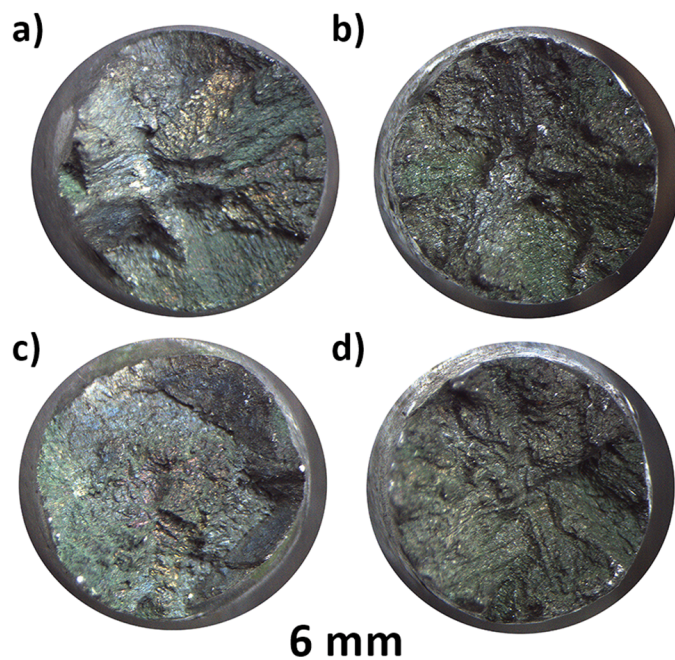


Fig. 9. Fractures of crept samples: a) N1; b) M1; c) N2; d) M2

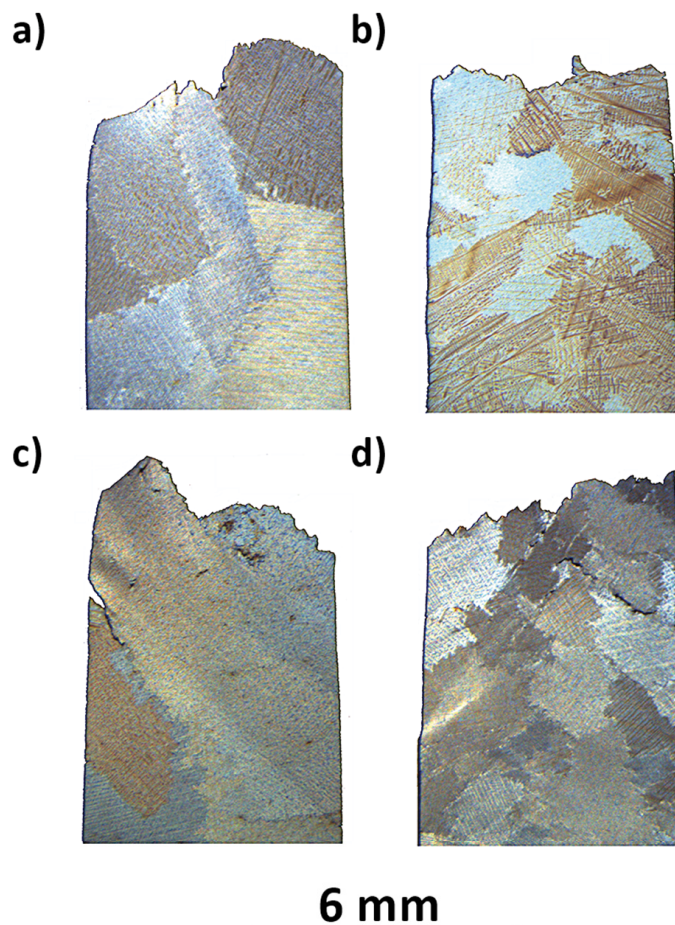


Fig. 10. Cross sections of crept samples: a) N1; b) M1; c) N2; d) M2

and also some which develop inwards from external areas. No cracks inside grains have been observed. The obtained results for all tested specimens reveal that time to rupture is longer than 30 h (average $t = 39.6$ h). Values meet the requirements of the industrial standards [17].

TABLE 6

Vickers hardness results

Description	N1	N2	M1	M2
Number of indent				
1	394.1	406.8	400.0	395.6
2	391.2	389.8	428.2	396.9
3	392.7	393.8	404.5	415.3
4	381.0	417.7	422.9	412.3
5	390.1	410.2	407.1	406.0
Mean value	389.8	403.7	412.5	405.2
Standard deviation	5.2	11.6	12.3	8.9

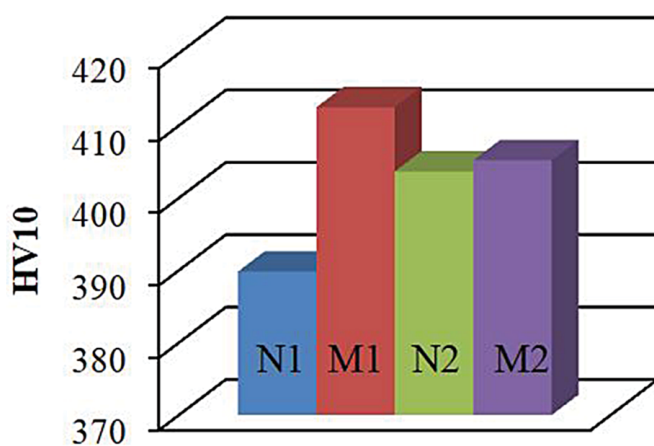


Fig. 11. Average Vickers hardness values for all investigated variants

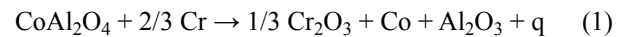
Vickers hardness test results with calculated mean values and standard deviations are shown in Table 5. The average values of the 5 measurements for each variant are graphically presented in Fig. 11. For both melt-pouring temperatures, the hardness average values in the modified samples were observed to increase. For lower temperature, the increase was almost 6%, while for the higher temperature for the unmodified and modified sample, the difference was only 1.5 HV, so it can be assumed that these values are very close (difference is within the measurement error limit).

4. Discussion

4.1. Macro and microstructure

Grain size depends primarily on velocity of growth and nucleation rate. In this work are considered two variants where preheat and melt-pouring temperature remain unchanged and so grain growth is constant. Refinement of the grains can be obtained via increment of the heterogeneous nucleation rate.

The fine-grained structure is related to a reaction between the alloying elements consisted in base metal and the inoculant. OES analysis reveals that IN-713C consists of highly reactive alloying elements like titanium, aluminum, as well as chromium. The oxide is reduced and metallic cobalt is formed according to the equations [18]:



These reactions are initiated by oxygen affinity of the aforementioned alloying elements. Cobalt in compound would be displaced by these elements to form Co fine particles, which are considered to be the relevant nucleants for surface grain refinement. Particles exist in melt-pouring temperature, Co is similar to Ni-rich γ phase both in crystallographic structure and lattice parameter. Cobalt and nickel have the same Face Centered Cubic system with $a_{\text{Co}} = 3.5547 \text{ \AA}$ and $a_{\text{Ni}} = 3.5805 \text{ \AA}$. Cobalt particles due to low lattice misfit with matrix can act as the nucleation substrata. Macrostructure observations did not revealed chill zones, which indicates that modification with the use of CoAl_2O_4 gives an exothermic reaction during pouring. Start of γ -matrix dendrite creation is pointed as 1342°C in turn solidification is finished at 1263°C . Inconel 713C has a wide range between liquidus and solidus (79°C) and so porosity is likely to form in its castings. Primary MC-type carbides that are responsible for increase of creep strength start to precipitate directly from liquid phase at 1305°C with a maximum at 1299°C . The main strengthening phase γ' is obtained as a product of transformation $\gamma \rightarrow \gamma'$ that occurs in a solid state in the temperature range 1169°C - 929°C . Precipitation of the γ' -phase from the γ solid solution starts near the eutectic areas and then occurs towards the dendrite cores during cooling. Near cubic shape of gamma prime particles indicates that the misfit coefficient is below $\pm 1\%$. Similar lattice parameters of γ and γ' makes that γ' nucleation energy is low and nucleating takes place under little supercooling. Hence, we observe a significant volume fraction of the γ' phase and consequent high mechanical properties in the as cast condition [15,19].

4.2. Influence of grain size on strength at ambient temperature

The size of the grains in a superalloy influences the strength because adjoining grains normally have different crystallographic orientations. The grain boundaries act as a barrier to dislocation movement for two reasons. Due to different orientation of two grains, a dislocation passing from one into the second grain will have to change its direction of motion. Secondly the atomic disorder within a grain boundary region will result in a discontinuity of slip planes from one grain into the other. A fine-grained alloy is harder and stronger than one that is coarse-grained, because has a greater grain boundaries area to hinder dislocation move-

ment. High strength also results from the high volume fraction of the coherent γ' particles, small width of the γ phase channels and the solid solution strengthening of γ and γ' phase [20]. Phase deformation of γ' occurs by slip on systems $\{111\} \langle 110 \rangle$. The dislocation in γ' phase has a Burger vector of length $a\sqrt{2}$, which is twice as long as in γ -matrix. Slip of a dislocation in the γ' phase by one length of the Burgers vector disrupts ordering of the crystal lattice. This creates an interface, which is a defect of high energy, so the dislocation movement in the γ' phase is much more difficult [21].

4.3. Influence of grain size on creep properties of Ni-based superalloy

Depending on the temperature and stress, there are three ranges in which creep mechanisms predominate. At high temperature/low stress (e.g. 982°C / 151.8 MPa) creep curve reveals a short primary stage and steady state represented by a plateau and pronounced strain appearing at the tertiary stage. In the case of superalloys and other alloys, two creep mechanisms are distinguished: dislocation creep (dislocation movement and climb) and diffusion creep [22]. The creep rate in both cases is dependent on the diffusion rate, so it fulfills the requirements of the Arrhenius equation. Taking into account the influence of grain size, the creep mechanisms can be divided into dependent and independent of its size. Dislocation creep that occurs inside the grains is independent of their size, while creep diffusion depends on the grain size, as vacancies form and disappear at the boundaries. With constant stress and temperature (as in this work) as the grain size increases, the contribution of dislocation creep goes down rapidly and decreases the creep rate via a diffusion mechanism. At a homologous temperature above 0.7 (in this paper 0.82), Nabarro-Herring creep prevails and occurs by migrating of vacancies inside grains from the stretched to the compressed regions and by the volume diffusion in the opposite direction. Below these temperatures, at a homologous temperature of 0.4-0.7 Coble creep that occurs through diffusion along grain boundaries prevails [20,23]. Creep rate via Nabarro-Herring mechanism is equal $1/d^2$, whereas via Coble is $1/d^3$. These relationships indicate that Coble creep is more strongly dependent on grain size than Nabarro-Herring creep, so that the contribution of the second mechanism will be much inconsiderable in fine-grained materials. Therefore, coarse grained nickel-alloys are characterized by higher creep resistance. Improvement of creep resistance can be achieved by solid solution and precipitation strengthening and also by grain boundary reduction or elimination.

5. Summary

Control of grain size in lost-wax casting is attained by control of manufacturing parameters like preheat and pouring temperature, together with the use of nucleants in prime coat

of the mould. The present research combines variants without and with addition of 5% cobalt aluminate and also two pouring temperatures namely 1480°C and 1520°C. The grains of superalloy castings can be refined to a considerable range by addition of the inoculant CoAl_2O_4 to the prime coat of moulds. The aim of inoculants is to produce during solidification of casting a large number of heterogeneous nucleation sites, which leads to an increase in the number of nucleating areas, so a numerous of crystals is created, which soon impinge on each other and preclude further growth. The influence of grain refinement on mechanical properties at elevated temperature and ambient temperature of Inconel 713C superalloy is analyzed. The research outcomes can be concluded as follows:

- 1) The highest refinement was observed in the modified sample poured at lower temperature (1480°C). The average surface of grain in specimen N1 with the prime coat that consisted zircon filler and colloidal silica binder is 6.42 mm² while the addition of CoAl_2O_4 decreases the average surface area above 2.5 times.
- 2) Grain refinement by addition of cobalt aluminate for specimens poured from both temperatures increase yield strength and hardness. Fine grain microstructure with high mechanical properties were obtained in as cast state. It is beneficial for elements like aerospace vanes clusters since they are mainly exposed to low cycle fatigue.
- 3) The creep resistance test indicated that all variants have favourable properties at 982°C with a mean time to fracture of nearly 40 h. Creep rate in the steady state depends strictly on grain size in both melt-pouring temperatures. In modified sample poured at 1480°C creep rate increases by more than 40% relative to non-modified sample, from 0.035% per hour to 0.050% per hour. In contrast, in specimens N2 and M2 creep rate slightly increases from 0.022 %/h to 0.025 %/h. Testing temperature was 0.82 of homologous temperature and so according to literature data Nabarro-Herring creep mechanism prevailed during testing.

Acknowledgments

This research work was supported by National Centre for Research and Development, Grant No. LIDER/227/L-6/14/NCBR/2015.

The authors wish to express appreciation to Prof. A.S. Wronski for the discussion and language correction of manuscript.

Conflicts of Interest

The authors declare no conflict of interest.

REFERENCES

- [1] R. Reed, *The Superalloys: Fundamentals and applications*, Cambridge University Press, Cambridge (2006).

- [2] Ł. Rakoczy et al., *Adv. in Mat. Sci.* **17** (2), 55-63 (2017) DOI: 10.1515/adms-2017-0011.
- [3] A. Chamanfar et al., *Mat. Sci. and Eng. A* **642**, 230-400 (2015) <http://dx.doi.org/10.1016/j.msea.2015.06.087>.
- [4] D. Laughlin, K. Hono, *Physical Metallurgy*, Elsevier (2014) <http://dx.doi.org/10.1016/B978-0-444-53770-6.00022-8>.
- [5] R. Ramesh et al., *J. Mat. Sci.* **27**, 270-278 (1992).
- [6] A. Royer et al., *Scr. Mat.* **40** (8), 955-961 (1991).
- [7] A. Szczotok, H. Matysiak, *J. of Mat. Eng. and Perform.* **23**, 2749-2759 (2014).
- [8] S. Roskosz, R. Cygan, *Inż. Mat.* **37** (2), 59-64 (2016).
- [9] P. Willemin, M. Durrand-Charre, *J. of Mat. Sci.* **25**, 168-174 (1990).
- [10] H. Matysiak et al., *JOM.* **68** (1), 185-197 (2015) <https://doi.org/10.1007/s11665-014-1123-4>
- [11] M. Zielińska, J. Sieniawski, *Arch. of Met. and Mat.* **58** (1), 95-98 (2013) <https://doi.org/10.2478/v10172-012-0157-6>.
- [12] T. Murakumo et al., "Superalloys" 155-62 (2004).
- [13] W. Jin, F. Bai, T. Li, G. Yin, *Mat. Let.* **62** 1585-1588 (2008) <http://dx.doi.org/10.1016/j.matlet.2007.09.028>.
- [14] Ł. Rakoczy, R. Cygan, Analysis of temperature distribution in shell mould during thin-wall superalloy casting and its effect on the resultant microstructure, *Arch. of Civ. and Mech. Eng.* **18**, 1441-1450 (2018). <https://doi.org/10.1016/j.acme.2018.05.008>.
- [15] H. Matysiak et al., *J. of Mat. Eng. and Perform.* **23** (9), 3305-3013 (2014). <https://doi.org/10.1007/s11665-014-1123-4>.
- [16] M. Azadi, M. Azadi, *Mat. Sci. and Eng.* **689** (24), 298-305 (2017).
- [17] https://www.nickelinstitute.org/~media/Files/TechnicalLiterature/Alloy713C_337_.ashx.
- [18] F. Jian, Y. Bin, *High Temperature Alloys for Gas Turbines: Investigation of the Surface Grain Refinement for Superalloys Castings*, Springer, Dordrecht (1982). https://doi.org/10.1007/978-94-009-7907-9_50.
- [19] F. Zupanic et al., *J. Alloy. Compd.* **329**, 290-297 (2001).
- [20] W.D. Callister, *Materials Science and Engineering*, John Wiley & Sons, New York (2007).
- [21] C.T. Liu, *Ordered Intermetallics: Physical Metallurgy and Mechanical Behaviour*, Springer Netherlands, Dordrecht (1992)
- [22] F. Nabarro, *The Physics of Creep*, Taylor and Francis, London (1995).
- [23] B. Burton, *J. of. Mat. Sci.* 4900-4903, (28) 1993.